Two-dimensional Heliocentric Dynamics Approximation of an Electric Sail with Fixed Attitude

Lorenzo Niccolai, Alessandro A. Quarta*, Giovanni Mengali

Department of Civil and Industrial Engineering, University of Pisa, I-56122 Pisa, Italy

Abstract

This work analyzes an approximate solution of the equations of motion for a spacecraft propelled by an Electric Solar Wind Sail with a fixed attitude. The peculiarity of such a propulsion system is that its thrust scales as the inverse heliocentric distance. This represents a substantial difference from a classical solar sail, whose propelling force is known to be proportional to inverse square distance from the Sun. Assuming a heliocentric, two-dimensional mission scenario, the polar form of the spacecraft trajectory equation is obtained for a closed parking orbit of given characteristics by means of an asymptotic expansion procedure. The proposed approach significantly improves the existing results as presented in the literature. A suitable choice of propulsion system parameters and parking orbit characteristics provides interesting similarities with recent solutions obtained for a solar sail-based spacecraft in a heliocentric, two-dimensional, mission scenario.

Keywords: Electric Solar Wind Sail, Asymptotic expansion method, Trajectory approximation, Generalized orbital elements

Nomenclature

$\mathbb{A}$,$\mathbb{B}$,$\mathbb{C}$,$\mathbb{D}$	=	matrices of coefficients
a	=	osculating orbit semimajor axis, [au]
a_c	=	spacecraft characteristic acceleration, [$\mathrm{mm/s^2}$]
b_i	=	dimensionless coefficients, see Eqs. (3)-(4)
E	=	dimensionless auxiliary variable, see Eq. (26)
e	=	osculating orbit eccentricity
h	=	osculating orbit specific angular momentum, [$\mathrm{au^2/day}$]
q_i	=	generalized orbital elements (with $\boldsymbol{q} \triangleq [q_1,\, q_2,\, q_3]^{\mathrm{T}}$)
$\boldsymbol{q}_j$	=	j-th perturbation order term of $\boldsymbol{q}$
R	=	dimensionless radial thrust
r	=	Sun-spacecraft distance, [au]
$r_\oplus$	=	reference distance, [au]
s	=	dimensionless auxiliary variable
T	=	dimensionless transverse thrust
$\mathcal{T}(O; r, \theta)$	=	polar reference frame
t	=	time, [days]
v_r	=	radial velocity, [au/day]
v_θ	=	transverse velocity, [au/day]

*Corresponding author

Email addresses: lorenzo.niccolai@ing.unipi.it (Lorenzo Niccolai), a.quarta@ing.unipi.it (Alessandro A. Quarta), g.mengali@ing.unipi.it (Giovanni Mengali)

Published in Aerospace Science and Technology, Vol. 71, December 2017, pp. 441–446. doi: https://doi.org/10.1016/j.ast.2017.09.045

α_n = E-sail pitch angle, [deg]
ϵ = relative error, see Eq. (27)
θ = angular coordinate, [deg]
$\mu_\odot$ = Sun's gravitational parameter, [$\mathrm{au}^3/\mathrm{day}^2$]
ω = apse line rotation angle, [deg]

Subscripts

0 = initial conditions
a = approximate results
max = maximum
n = numerical results

Superscripts

$\tilde{}$ = dimensionless
$\dot{}$ = time derivative

1. Introduction

The trajectory analysis of a spacecraft propelled by a low-thrust propulsion system usually requires the equations of motion to be integrated numerically. This approach implies a non-negligible computational cost, especially in a preliminary mission design, where a number of different scenarios must be analyzed. In this context, the availability of an analytical approximation of the spacecraft trajectory is therefore an useful analysis tool.

Recently, Niccolai et al. [1] have discussed an analytical approximate model for the dynamics of a solar sail-based spacecraft with a fixed attitude, assuming a two-dimensional heliocentric mission scenario. Using such a propulsion system, the propulsive thrust varies as the inverse square distance from the Sun. An accurate approximation of the spacecraft (propelled) trajectory is obtained in Ref. [1] with the help of the following two aids: 1) the state of the vehicle is characterized by the set of non-singular generalized orbital elements introduced by Bombardelli et al. [2], and 2) the problem is addressed with an asymptotic expansion procedure [3, 4].

The aim of this work is to extend the results discussed in Ref. [1] to the case in which the spacecraft primary propulsion system is an Electric Solar Wind Sail (E-sail). The E-sail concept has been proposed by Pekka Janhunen in 2004 [5]. It is a propellantless propulsion system (such as solar sail) and consists of a spinning grid of tethers that are kept at a high potential by an onboard electron gun. When the grid is immersed in the solar wind, the charged tethers interact with the incoming ions, and the momentum exchange generates a continuous propulsive acceleration whose modulus varies with the spacecraft attitude [6, 7, 8], and, unlike the solar sail case, it scales with the inverse heliocentric distance [9].

The dynamics of an E-sail-based spacecraft will now be described with an approach formally similar to that presented in Ref. [1]. Notably, some significant results available for solar sails are shown to apply to E-sails as well. At the same time, the approximate models currently available in the literature [10] are substantially improved without the need of significant additional computational costs. Unlike the method of Ref. [10], the new model can be applied to a generic (closed) parking orbit. This is an important point, since the spacecraft usually starts its interplanetary mission from a circular or elliptic parking orbit and then exploits the E-sail propulsive thrust in order to change the orbital elements and meet the mission requirements. Finally, the implementation of a rectification procedure, which improves the results accuracy, allows possible (instantaneous) sail attitude variations during the flight to be simulated.

2. Two-dimensional E-sail Heliocentric Dynamics

Consider an E-sail-based spacecraft that initially covers a closed heliocentric parking orbit with semimajor axis a_0 and eccentricity $e_0 < 1$. Let a_c be the spacecraft characteristic acceleration, that is, the maximum propulsive acceleration modulus at a Sun-spacecraft distance $r = r_\oplus \triangleq 1\,\mathrm{au}$, which represents the typical E-sail performance parameter [11, 12, 13]. Assuming a two-dimensional propelled trajectory belonging to

the parking orbit plane, the spacecraft equations of motion in a heliocentric polar reference frame $\mathcal{T}(O; r, \theta)$ are

$$\ddot{r} - r\,\dot{\theta}^2 = -\frac{\mu_\odot}{r^2} + a_c \left(\frac{r_\oplus}{r}\right) R \tag{1}$$

$$r\,\ddot{\theta} + 2\,\dot{r}\,\dot{\theta} = a_c \left(\frac{r_\oplus}{r}\right) T \tag{2}$$

where $\mu_\odot$ is the Sun's gravitational parameter, θ is the spacecraft angular coordinate measured counterclockwise with respect to the direction of the parking orbit eccentricity vector $\boldsymbol{e}_0$, and R (or T) is the radial (or transverse) component of the dimensionless local propulsive acceleration vector. According to Yamaguchi and Yamakawa [6, 7], R and T are functions of the sail pitch angle $\alpha_n \in [-90,\, 90]$ deg. The latter, see Fig. 1, is defined as the angle between the Sun-spacecraft line and the unit vector normal to the E-sail nominal plane in the direction opposite to the Sun.

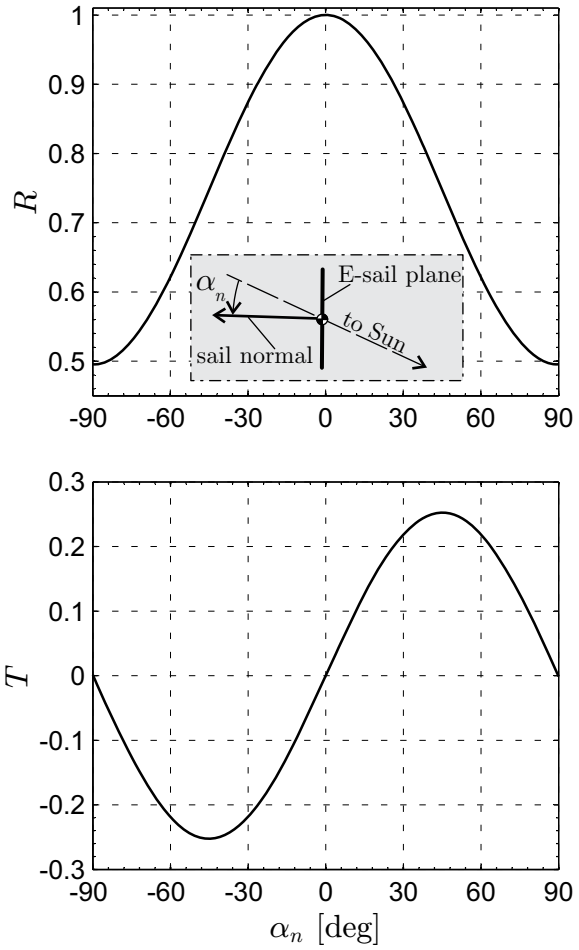

Figure 1: Radial (R) and transverse (T) component of the dimensionless propulsive acceleration as functions of the sail pitch angle α_n. Data adapted from Refs. [6, 7].

An useful approximation of $R = R(\alpha_n)$ and $T = T(\alpha_n)$ is given in Ref. [8]

$$R \simeq b_1 + b_2 \, \cos(2\,\alpha_n) \tag{3}$$

$$T \simeq b_2 \, \sin(2\,\alpha_n) \tag{4}$$

where $b_1 \simeq 0.7477$ and $b_2 \simeq 0.2523$ are dimensionless coefficients obtained through a best-fit procedure. Recently, Huo et al. [14], through a geometrical analysis of the E-sail thrust vector based on the work of Toivanen and Janhunen [15, 16], have demonstrated that the expressions of $R = R(\alpha_n)$ and $T = T(\alpha_n)$ given by Eqs. (3)-(4) are exact when $b_1 = 3/4$ and $b_2 = 1/4$.

Equations (3) and (4) show important differences between the thrust behavior of an E-sail compared to that of a more conventional solar sail, besides the different way with which the propulsive force scales with the heliocentric distance. In fact, for a solar sail, the expressions of the dimensionless propulsive acceleration components $R_{\rm ss}$ and $T_{\rm ss}$ can be expressed as functions of the pitch angle α_n as $R_{\rm ss} = \cos\alpha_n(c_1 + c_2 \, \cos^2 \, \alpha_n + c_3 \, \cos\alpha_n)$ and $T_{\rm ss} = \cos\alpha_n \, \sin\alpha_n \, (c_2 \, \cos\alpha_n + c_3)$, where the c_i coefficients depend on the solar sail optical properties and the thrust model adopted [17].

According to Bombardelli et al. [2], the spacecraft state vector can be described in terms of the dimensionless modified non-singular orbital elements $\{q_1, q_2, q_3\}$ defined as

$$q_1 = \frac{e}{\widetilde{h}} \, \cos\omega \quad , \quad q_2 = \frac{e}{\widetilde{h}} \, \sin\omega \quad , \quad q_3 = \frac{1}{\widetilde{h}} \tag{5}$$

where e is the osculating orbit eccentricity, ω is the angle between the direction of $\boldsymbol{e}_0$ and the direction of the osculating orbit eccentricity vector, and $\widetilde{h}$ is the dimensionless angular momentum modulus of the osculating orbit. The latter can be calculated as a function of the semilatus rectum p of the osculating orbit as $\widetilde{h} \triangleq \sqrt{p/r_0}$, being $r_0 \triangleq r(t_0)$ the Sun-spacecraft distance at the initial time $t_0 \triangleq 0$. Accordingly, Eqs. (1)-(2) can be rewritten in a vectorial form [2] as

$$\frac{\mathrm{d}\boldsymbol{q}}{\mathrm{d}\theta} = \widetilde{a}_c \, \mathbb{A} \, \widetilde{\boldsymbol{a}} \qquad \text{with} \qquad \mathbb{A} \triangleq \frac{1}{q_3 \, s^2} \begin{bmatrix} s \, \sin\theta & (s+q_3) \, \cos\theta \\ -s \, \cos\theta & (s+q_3) \, \sin\theta \\ 0 & -q_3 \end{bmatrix} \tag{6}$$

where $\boldsymbol{q} \triangleq [q_1, \, q_2, \, q_3]^{\rm T}$ is the spacecraft state vector in terms of dimensionless non-singular orbital elements, $\widetilde{\boldsymbol{a}} \triangleq [R, \, T]^{\rm T}$ is the dimensionless propulsive acceleration vector, $s \triangleq (q_1 \, \cos\theta + q_2 \, \sin\theta + q_3)$ is an auxiliary variable, and

$$\widetilde{a}_c = \frac{a_c}{\mu_\odot / r_0^2} \left(\frac{r_\oplus}{r_0} \right) \tag{7}$$

is a sort of dimensionless characteristic acceleration, whose value depends on the initial Sun-spacecraft distance $r_0 = a_0(1 - e_0^2)/(1 + e_0 \, \cos\theta_0)$, calculated at $\theta = \theta_0 \triangleq \theta(t_0)$. The first order vectorial differential equation (6) is completed by the initial conditions $\boldsymbol{q}_0 \triangleq \boldsymbol{q}(\theta_0)$ evaluated on the parking orbit. Since $\omega(t_0) = 0$, and recalling Eqs. (5), the vector $\boldsymbol{q}_0$ becomes

$$\boldsymbol{q}_0 = \frac{1}{\sqrt{1 + e_0 \, \cos\theta_0}} \, [e_0, \, 0, \, 1]^{\rm T} \tag{8}$$

The Sun-spacecraft distance (r), and the radial (v_r) and transverse (v_θ) components of the spacecraft inertial velocity may be expressed as functions of the modified parameters [2] as

$$r = \frac{r_0}{q_3^2 + q_1 \, q_3 \, \cos\theta + q_2 \, q_3 \, \sin\theta} \tag{9}$$

$$v_r \triangleq \dot{r} = \sqrt{\frac{\mu_\odot}{r_0}} \, (q_1 \, \sin\theta - q_2 \, \cos\theta) \tag{10}$$

$$v_\theta \triangleq r \, \dot{\theta} = \sqrt{\frac{\mu_\odot}{r_0}} \, (q_1 \, \cos\theta + q_2 \, \sin\theta + q_3) \tag{11}$$

Using Eqs. (5) and Eqs. (9)-(11), the evaluation of the classical orbital elements as functions of the modified parameters is straightforward. However, the corresponding expressions are here omitted for the sake of conciseness, and the interested reader is referred to Ref. [2].

Paralleling the procedure described in Ref. [1], an interesting analytical approximation of the solution to the differential system of Eqs. (6) and (8) can be obtained when $\widetilde{a}_c \ll 1$ and $\{R,\, T\}$ are constants of motion. Bearing in mind Eq. (7), the assumption $\widetilde{a}_c \ll 1$ is consistent with a low-performance E-sail, that is, an E-sail whose propulsive acceleration modulus is significatively smaller than the Sun's (local) gravitational acceleration. Moreover, the assumption that both R and T are constants of motion is consistent with a case in which the E-sail maintains a fixed attitude (i.e. a constant pitch angle, see Fig. 1) with respect to an orbital reference frame.

2.1. Approximate analytical solution

As long as $\widetilde{a}_c \ll 1$, the E-sail propulsive acceleration can be considered as a perturbation of the spacecraft Keplerian motion. Accordingly, the modified orbital parameters can be written by means of an asymptotic series expansion [1, 2, 4] as

$$\boldsymbol{q} = \boldsymbol{q}_0 + \widetilde{a}_c\, \boldsymbol{q}_1 + O(\widetilde{a}_c^2) \tag{12}$$

where $\boldsymbol{q}_1$ represents the first order perturbative term of the spacecraft state vector $\boldsymbol{q}$. Higher order perturbation terms are neglected in the rest of the work, i.e. $O(\widetilde{a}_c^2) \simeq 0$, since an analytical solution that reduces the computational costs cannot be obtained when second (or higher) order perturbative terms are included in the analysis.

When Eq. (12) is substituted into Eq. (6), the vectorial differential equation involving $\boldsymbol{q}_1$ is obtained by equating the terms proportional to $\widetilde{a}_c$ [2], viz.

$$\frac{\mathrm{d}\boldsymbol{q}_1}{\mathrm{d}\theta} = \mathbb{B}\,\widetilde{\boldsymbol{a}} \qquad \text{with} \qquad \boldsymbol{q}_1(\theta_0) \triangleq 0 \tag{13}$$

where

$$\mathbb{B} \triangleq \frac{\sqrt{1+e_0\,\cos\theta_0}}{1+e_0\,\cos\theta} \begin{bmatrix} \sin\theta & \cos\theta \left(\dfrac{2+e_0\,\cos\theta}{1+e_0\,\cos\theta}\right) \\ -\cos\theta & \sin\theta \left(\dfrac{2+e_0\,\cos\theta}{1+e_0\,\cos\theta}\right) \\ 0 & -\dfrac{1}{1+e_0\,\cos\theta} \end{bmatrix} \tag{14}$$

Since $\{R,\, T\}$ are constants of motion, the term $\widetilde{\boldsymbol{a}}$ in Eq. (13) is a constant vector whose components depend on the value of the constant pitch angle, see Fig. 1 or Eqs. (3)-(4). Note that Eq. (13) is formally similar to Eq. (29) of Ref. [1], which refers to a solar sail-based mission case, the main difference being that the components of matrix $\mathbb{B}$ now contain terms proportional to $(1+e_0\,\cos\theta)^{-2}$. However, in the noteworthy case of circular parking orbit ($e_0 = 0$), Eqs. (13)-(14) coincide with those obtained in Ref. [1].

Equation (13) can be integrated with respect to the angular variable θ, distinguishing according to whether the parking orbit is circular or elliptical ($e_0 \neq 0$). In case of circular parking orbit, the angular coordinate θ and the angle ω are measured from a generic (fixed) direction, so that $\theta_0 = 0$ can be assumed without loss of generality. Taking into account Eq. (14), when $e_0 = 0$ the solution of Eq. (13) is

$$\boldsymbol{q}_1 = \mathbb{C}\,\widetilde{\boldsymbol{a}} \qquad \text{with} \qquad \mathbb{C} \triangleq \begin{bmatrix} (1-\cos\theta) & 2\,\sin\theta \\ -\sin\theta & 2\,(1-\cos\theta) \\ 0 & -\theta \end{bmatrix} \tag{15}$$

Therefore, according to Eqs. (8) and (12), the variation of $\boldsymbol{q}$ with the angular coordinate θ is given by the following (approximate) equation

$$\boldsymbol{q} \simeq [0,\, 0,\, 1]^{\mathrm{T}} + \widetilde{a}_c\, \mathbb{C}\,\widetilde{\boldsymbol{a}} \tag{16}$$

In particular, having $q_3 > 0$ for physical reasons (see the last of Eqs. (5)), a maximum value exists for the angular coordinate, that is, $\max(\theta) \triangleq \theta_{\max} = 1/(T\,\widetilde{a}_c)$, beyond which the approximate solution (16) cannot be applied. Figure 2 shows how $\theta_{\max}$ varies with the E-sail attitude and the characteristic acceleration evaluated with $r_0 = r_\oplus$.

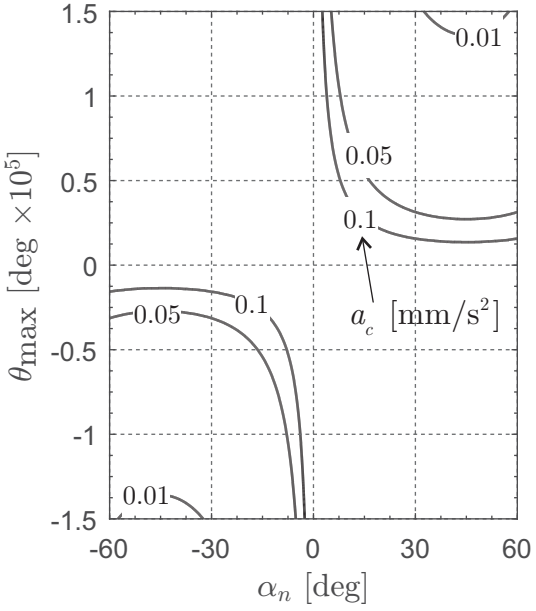

Figure 2: Maximum angular coordinate $\theta_{\max}$ for the circular parking orbit case ($r_0 = r_\oplus$) as a function of the E-sail pitch angle α_n and the characteristic acceleration a_c.

Assuming $\theta < \theta_{\max}$, the polar equation of the spacecraft trajectory and the spacecraft inertial velocity components may be obtained by substituting the components of $\boldsymbol{q}$ given by Eq. (16) into Eqs. (9)-(11), viz.

$$r = \frac{r_0}{(1 - T\,\widetilde{a}_c\,\theta)\,[1 + R\,\widetilde{a}_c\,(\cos\theta - 1) + T\,\widetilde{a}_c\,(2\,\sin\theta - \theta)]} \tag{17}$$

$$v_r = \sqrt{\frac{\mu_\odot}{r_0}}\,\widetilde{a}_c\,[2\,T\,(1 - \cos\theta) + R\,\sin\theta] \tag{18}$$

$$v_\theta = \sqrt{\frac{\mu_\odot}{r_0}}\,\left[1 - 2\,R\,\widetilde{a}_c\,\sin^2(\theta/2) + T\,\widetilde{a}_c\,(2\sin\theta - \theta)\right] \tag{19}$$

Note that Eqs. (17)-(19) coincide with the results obtained in Ref. [1], provided the solar sail lightness number (β) be formally substituted with the E-sail dimensionless characteristic acceleration $\widetilde{a}_c$. This implies that the heliocentric behaviours of two different (propellantless) propulsion systems, such as the solar sail and the E-sail, are, to a first order, similar when the parking orbit is circular, the motion is two-dimensional and the sail pitch angle is maintained constant.

For an elliptic parking orbit ($e_0 \neq 0$), the initial angular coordinate θ_0 coincides with the true anomaly on the osculating orbit at $t = t_0$. In this case the integration of Eqs. (13) is more involved, but it can be verified that

$$\boldsymbol{q} \simeq \boldsymbol{q}_0 + \mathbb{D}\,\widetilde{\boldsymbol{a}} \qquad \text{with} \qquad \mathbb{D} \triangleq \begin{bmatrix} D_{11} & D_{12} \\ D_{21} & D_{22} \\ 0 & D_{32} \end{bmatrix} \tag{20}$$

where $\boldsymbol{q}_0$ is given by Eq. (8) and

$$D_{11} \triangleq -\frac{\widetilde{a}_c\,\widetilde{h}_0}{e_0}\,\ln\left(\frac{1+e_0\,\cos\theta}{\widetilde{h}_0^2}\right) \tag{21}$$

$$D_{12} \triangleq \widetilde{a}_c\,\widetilde{h}_0\,\left[\frac{\theta-\theta_0}{e_0} - \frac{E-E_0}{e_0\,\sqrt{(1-e_0^2)^3}} + \frac{1}{1-e_0^2}\left(\frac{\sin\theta}{1+e_0\,\cos\theta} - \frac{\sin\theta_0}{\widetilde{h}_0^2}\right)\right] \tag{22}$$

$$D_{21} \triangleq -\frac{\widetilde{a}_c\,\widetilde{h}_0}{e_0}\left(\theta-\theta_0-\frac{E-E_0}{\sqrt{1-e_0^2}}\right) \tag{23}$$

$$D_{22} \triangleq -\frac{\widetilde{a}_c\,\widetilde{h}_0}{e_0}\left[\ln\left(\frac{1+e_0\,\cos\theta}{\widetilde{h}_0^2}\right) - \frac{1}{1+e_0\,\cos\theta} + \frac{1}{\widetilde{h}_0^2}\right] \tag{24}$$

$$D_{32} \triangleq -\frac{\widetilde{a}_c\,\widetilde{h}_0}{1-e_0^2}\left[\frac{E-E_0}{\sqrt{1-e_0^2}} - \frac{2\,e_0\,\tan(\theta/2)}{(1-e_0)\,\tan^2(\theta/2)+1+e_0} + \frac{2\,e_0\,\tan(\theta_0/2)}{(1-e_0)\,\tan^2(\theta_0/2)+1+e_0}\right] \tag{25}$$

with $\widetilde{h}_0 \triangleq \widetilde{h}(t_0) = \sqrt{1+e_0\,\cos\theta_0}$, and E is an auxiliary dimensionless variable defined as

$$E \triangleq 2\,\arctan\left(\sqrt{\frac{1-e_0}{1+e_0}}\,\tan\frac{\theta}{2}\right) \tag{26}$$

Finally, the analytical polar form of the trajectory equation can be obtained by substituting the components of Eq. (20) into Eq. (9). The final result is here omitted for the sake of conciseness.

The error introduced by the asymptotic series approximation increases for large values of the pair $\{\widetilde{a}_c,\,\theta\}$. However, it is possible to improve the model accuracy by means of a rectification procedure, introduced in Ref. [2] and discussed in depth in Ref. [1]. More specifically, the rectification procedure consists of updating the initial conditions and the fixed direction from which the angles θ and ω are measured at a given time instant. The use of a rectification procedure reduces the error in terms of difference between the analytical and the simulation results, but increases the computational costs. Note that instantaneous sail attitude variations (i.e. variations of the components of the vector $\widetilde{\boldsymbol{a}}$) can be easily introduced in the rectification points, thus improving the overall model flexibility.

2.2. Model validation

The accuracy of the proposed (approximate) model has been checked by direct comparison with the results obtained by a numerical integration of the equations of motion in double precision, using a variable order Adams-Bashforth-Moulton solver scheme [18, 19] with absolute and relative errors of 10^{-12}.

The first test case example involves a circular parking orbit with $a_0 \equiv r_0 = r_\oplus$, that is, a mission case consistent with a spacecraft leaving the Earth's sphere of influence with zero hyperbolic excess speed. Paralleling the procedure described in Ref. [1], the difference in terms of Sun-spacecraft distance r between the analytical approximation (without rectification) and the numerical results (subscript n) may be quantified through the relative error ϵ defined as

$$\epsilon \triangleq \max_{\theta}\left(\frac{|r_n(\theta)-r(\theta)|}{r_0}\right) \tag{27}$$

Figure 3 shows that, even without any rectification procedure, ϵ is smaller than 4% for a simulation time of 5 years and $a_c \le 0.1\,\mathrm{mm/s^2}$ (which corresponds to a low-performance E-sail). Note that, in this case $\widetilde{a}_c \simeq a_c/(5.93\,\mathrm{mm/s^2})$, see Eq. (7).

A similar estimation of the differences between the analytical method and the numerical integration is now given for the elliptic parking orbit case. The selected initial orbital parameters are $a_0 = a_☿ = 0.308\,\mathrm{au}$, $e_0 = e_☿ = 0.206$, and $\nu_0 = 0$. This situation simulates the exit from Mercury's sphere of influence at the

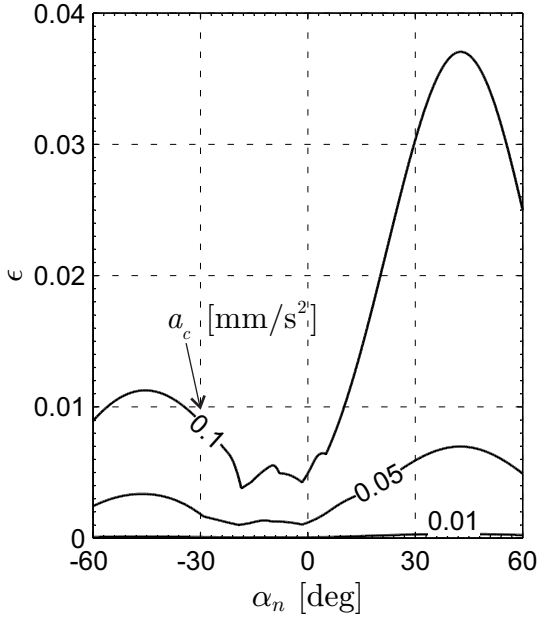

Figure 3: Relative error ϵ as a function of α_n and a_c for a simulation time of 5 years ($e_0 = 0$ and $a_0 = r_\oplus$).

planetary perihelion with zero hyperbolic excess speed. For a simulation time of 5 years, Fig. 4 shows that the error ϵ is smaller than 10%, and is appreciable only for large values of pitch angle and characteristic acceleration. These results confirm the flexibility of the approximation, whose performance is good both for a circular and an elliptical parking orbit, and suggest that rectification procedures are advisable especially in the elliptic parking orbit case.

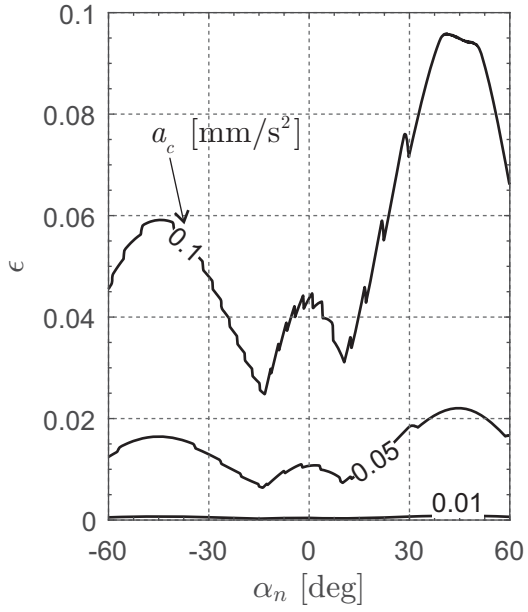

Figure 4: Relative error ϵ as a function of α_n and a_c for a simulation time of 5 years ($e_0 = e_{\mathrm{☿}}$, $a_0 = a_{\mathrm{☿}}$), and $\nu_0 = 0$.

3. Comparison with the Literature Results

The results of the proposed method are now compared with the analytical approximation of the E-sail heliocentric dynamics given by Ref. [10]. In particular, the model of Ref. [10] is obtained by neglecting the radial acceleration ($\ddot{r}$) in the equations of motion, and is based on the three following assumptions: 1) the trajectory is two-dimensional; 2) the E-sail has a fixed attitude; 3) the parking orbit is circular. Recall that the model discussed in this work is more general than that of Ref. [10] since it can be applied to a closed parking orbit, that is, when $e_0 < 1$.

For illustrative purposes, consider a 10 years orbit raising from a circular parking orbit of radius $r_0 = r_\oplus$ using an E-sail with a characteristic acceleration $a_c = 0.1\,\mathrm{mm/s^2}$. According to Ref. [10], and bearing in mind the results of Refs. [6, 7], assume a pitch angle $\alpha_n = 45\,\mathrm{deg}$, that is, a pitch angle that maximizes the transverse component of the dimensionless propulsive acceleration T, see Fig. 1. Figures 5 and 6 show the time variations of $\{r, v_r, v_\theta\}$, and the osculating orbit parameters calculated with a numerical integration (solid line), using the approximate method of Ref. [10] (dash line), and the proposed analytical method (dash-dot line) with one rectification every six months. The corresponding spacecraft (polar) trajectory is shown in Fig. 7. Note that the analytical method of Ref. [10] is quite accurate in predicting the secular variations of the spacecraft osculating orbit parameters. However, the proposed model is superior in terms of capability of accurately evaluating the short-term oscillations. When coupled with a rectification procedure, it also shows an overall better performance with respect to the model of Ref. [10] while maintaining a moderate computational cost. In fact, in our simulations (with two rectifications per year), the time saving is about two order of magnitudes when compared to a numerical integration approach.

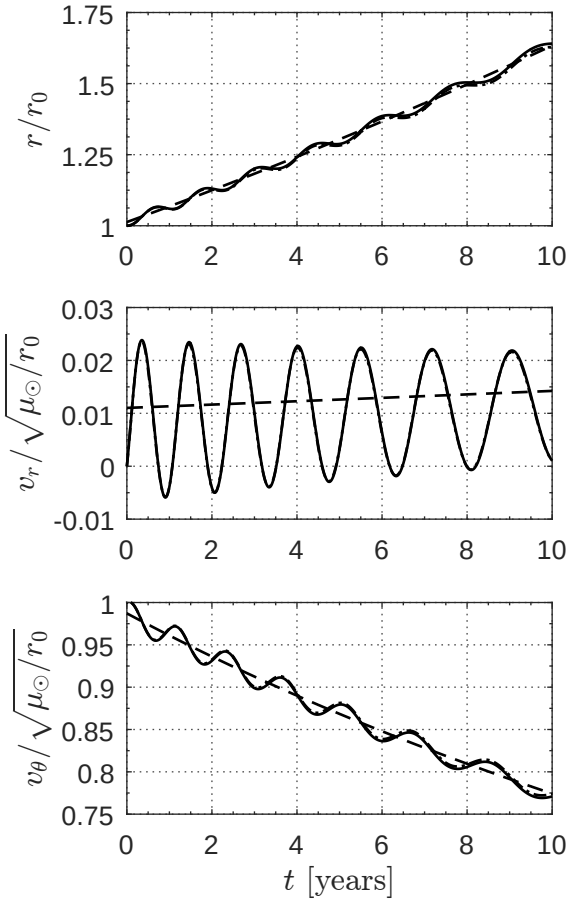

Figure 5: Results for a 10 years orbit raising with $a_c = 0.1\,\mathrm{mm/s^2}$, $\alpha_n = 45\,\mathrm{deg}$, $r_0 = r_\oplus$, and $e_0 = 0$ (solid line = numerical integration; dash line = analytical method of Ref. [10]; dash-dot line = proposed analytical method with 19 rectifications).

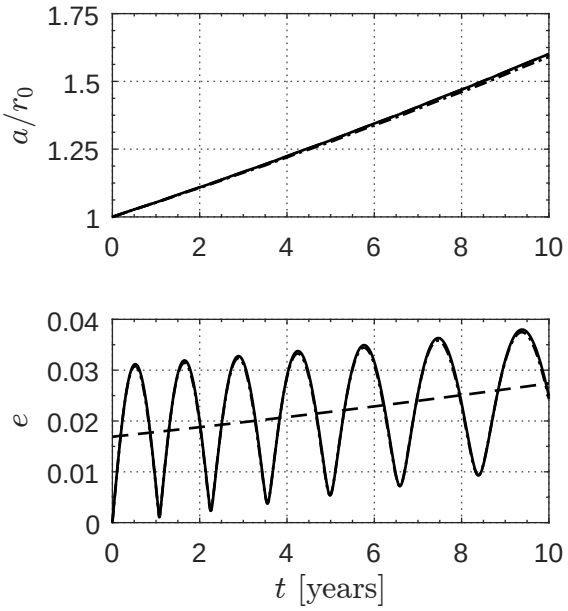

Figure 6: Osculating orbit parameter time evolution for a 10 years orbit raising with $a_c = 0.1\,\mathrm{mm/s^2}$, $\alpha_n = 45\,\mathrm{deg}$, $r_0 = r_\oplus$, and $e_0 = 0$ (solid line = numerical integration; dash line = analytical method of Ref. [10]; dash-dot line = proposed analytical method with 19 rectifications).

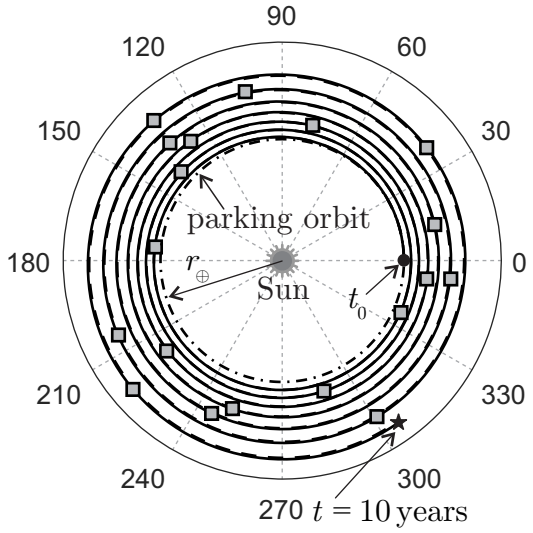

Figure 7: Spacecraft trajectory during a 10 years orbit raising with $a_c = 0.1\,\mathrm{mm/s^2}$, $\alpha_n = 45\,\mathrm{deg}$, $r_0 = r_\oplus$, $e_0 = 0$ (solid line = numerical integration; dash line = approximate model with 19 rectifications; square = rectification point).

4. Conclusions

An analytical approximate solution for the two-dimensional equations of motion of a spacecraft propelled by a Electric Solar Wind Sail has been discussed. The mathematical method used to obtain the approximation is based on the procedure applied in a recent work focusing on solar sail-based spacecraft, but the different relation between the propulsive thrust and the heliocentric distance produces new and significant outcomes. The obtained results guarantee a substantial reduction of the computational costs when compared to a numerical integration of the equations motion. The possibility of including a rectification procedure

improves the method accuracy, and allows the designer to model possible sail attitude variations during the flight. A comparison with a previous (approximate) method confirms the new model to show significant improvements in terms of results accuracy and flexibility. Indeed, the procedure discussed in this work can be applied also in case of elliptical parking orbit and is capable of predicting not only the secular variation of the orbital parameters, but also their short-term oscillations.

Conflict of interest statement

The authors declared that they have no conflicts of interest to this work.

References

[1] L. Niccolai, A. A. Quarta, G. Mengali, Solar sail trajectory analysis with asymptotic expansion method, Aerospace Science and Technology 68 (2017) 431–440, doi: 10.1016/j.ast.2017.05.038.

[2] C. Bombardelli, G. Baú, J. Peláez, Asymptotic solution for the two-body problem with constant tangential thrust acceleration, Celestial Mechanics and Dynamical Astronomy 110 (3) (2011) 239–256, doi: 10.1007/s10569-011-9353-3.

[3] J. Kevorkian, The two-variable expansion procedure for the approximate solution of certain non-linear differential equations, Vol. 7, American Mathematical Society, 1966.

[4] W. Stavro, Low-thrust trajectories using the two variable asymptotic expansion method, Master's thesis, California Institute of Technology (1969).

[5] P. Janhunen, Electric sail for spacecraft propulsion, Journal of Propulsion and Power 20 (4) (2004) 763–764, doi: 10.2514/1.8580.

[6] K. Yamaguchi, H. Yamakawa, Study on orbital maneuvers for electric sail with on-off thrust control, Aerospace Technology Japan, the Japan Society for Aeronautical and Space Sciences 12 (2013) 79–88, doi: 10.2322/astj.12.79.

[7] K. Yamaguchi, H. Yamakawa, Electric solar wind sail kinetic energy impactor for near earth asteroid deflection mission, The Journal of the Astronautical Sciences 63 (1) (2016) 1–22, doi: 10.1007/s40295-015-0081-x.

[8] A. A. Quarta, G. Mengali, Minimum-time trajectories of electric sail with advanced thrust model, Aerospace Science and Technology 55 (2016) 419–430, doi: 10.1016/j.ast.2016.06.020.

[9] P. Janhunen, The electric solar wind sail status report, in: European Planetary Science Congress 2010, Vol. 5, European Planetology Network and the European Geosciences Union, 2010, paper EPSC 2010-297.

[10] A. A. Quarta, G. Mengali, Trajectory approximation for low-performance electric sail with constant thrust angle, Journal of Guidance, Control, and Dynamics 36 (3) (2013) 884–887, doi: 10.2514/1.59076.

[11] G. Mengali, A. A. Quarta, P. Janhunen, Electric sail performance analysis, Journal of Spacecraft and Rockets 45 (1) (2008) 122–129, doi: 10.2514/1.31769.

[12] A. A. Quarta, G. Mengali, P. Janhunen, Optimal interplanetary rendezvous combining electric sail and high thrust propulsion system, Acta Astronautica 68 (5-6) (2011) 603–621, doi: 10.1016/j.actaastro.2010.01.024.

[13] P. Janhunen, A. A. Quarta, G. Mengali, Electric solar wind sail mass budget model, Geoscientific Instrumentation, Methods and Data Systems 2 (1) (2013) 85–95, doi: 10.5194/gi-2-85-2013.

[14] M. Huo, G. Mengali, A. A. Quarta, Electric sail thrust model from a geometrical perspective, In press. Journal of Guidance, Control, and Dynamics .

[15] P. Toivanen, P. Janhunen, Spin plane control and thrust vectoring of electric solar wind sail, Journal of Propulsion and Power 29 (1) (2013) 178–185, doi: 10.2514/1.B34330.

[16] P. Toivanen, P. Janhunen, Thrust vectoring of an electric solar wind sail with a realistic sail shape, Acta Astronautica 131 (2017) 145–151, doi: 10.1016/j.actaastro.2016.11.027.

[17] C. R. McInnes, Solar Sailing: Technology, Dynamics and Mission Applications, Space Science and Technology, Springer-Verlag, Berlin, 2004, pp. 47–50, ISBN: 978-3540210627.

[18] L. F. Shampine, M. K. Gordon, Computer Solution of Ordinary Differential Equations: The Initial Value Problem, W. H. Freeman, San Francisco, 1975, Ch. 10.

[19] L. F. Shampine, M. W. Reichelt, The MATLAB ODE suite, SIAM Journal on Scientific Computing 18 (1) (1997) 1–22, doi: 10.1137/S1064827594276424.